Available online at www.sciencedirect.com
ScienceDirect
Catalysis Today 118 (2006) 32–38
CATALYSIS TODAY
www.elsevier.com/locate/cattod

Heat transfer studies in an inorganic membrane reactor at pilot plant scale

Mónica Alonso [a], Gregory Patience [b,*], José Ramón Fernández [a], María Jesús Lorences [c], Fernando Díez [a], Aurelio Vega [a], Roberta Cenni [c]

[a] *Department Chem. Eng., University of Oviedo, Julián Clavería 33007 Oviedo, Spain*
[b] *Ecole Polytechnique Montreal, CP 6079, Succ. CV, Quebec, Canada H3C 3A7*
[c] *Haldor Topsoe A/S, Nymollevej 55, Lyngby, Denmark*

Available online 21 July 2006

Abstract

The partial oxidation of butane to maleic anhydride over VPO catalyst was used to compare heat transfer in a conventional fixed bed and an inorganic membrane reactor. Three resistances to heat transfer were studied: internal resistance from the inner wall of the reactor to the fluid, heat conduction/convection across the wall and the resistance between the fluid bed and outer wall. The overall heat transfer coefficient measured in the reactor operating as a conventional fixed bed was 100 W/m^2 K, which was an order of magnitude greater than that measured in the membrane reactor configuration. This large difference was attributed to the heat transfer resistance between the interior tube wall and the fluid: gas permeating across the membrane tube may have created a boundary layer thus limiting the mixing between the two fluids. Doubling the Reynolds number appeared to improve the heat transfer rate in the membrane reactor substantially, such that it approached the performance of the conventional fixed bed. Based on correlations in the literature, this large improvement in the heat transfer rate was unexpected.

Keywords: Pilot plant inert membrane reactor; Fluidized bed; Butane oxidation; Maleic anhydride; VPO catalyst; Heat transfer

1. Introduction

Due to their functional qualities, membrane reactors have been considered for partial oxidation reactions by several research groups [1–5]. Not only are these reactors inherently safer to operate, they claim that when the oxygen is distributed axially along the bed, the selectivity is higher since the average oxygen concentration in the reaction zone is lower. For a parallel reaction network, this observation is true when the reaction order of oxygen is higher for the parasitic reaction compared to the selective reaction [6]. In an earlier study [7], we showed that the temperature profile was flatter in a membrane reactor compared to a fixed bed for a given production rate (assuming the heat transfer coefficients of the two reactor types were equal). The flatter temperature profile implied that higher feed rates were possible resulting in increased production.

Several limitations of membrane reactors have been cited recently [8–10]. These studies have shown that higher product yields were attained due to the longer contact times resulting in increased conversion. The membrane reactor selectivity was not necessarily as high as in a fixed bed operating under similar conditions. Selectivities equivalent to those measured in a fixed bed were achieved only at lower temperatures. Furthermore, it has been recognized [11,12] that under conditions where the oxygen feed is distributed, the catalyst oxidation state may vary both radially and axially in the reactor, resulting in sub-optimal selectivity. As the best catalyst for the fixed bed is not necessarily the best catalyst for a membrane reactor, a comparison of the two technologies based on the same catalyst may be unfair. Particularly for the VPO catalyst used in butane oxidation to maleic anhydride, it has been demonstrated that vanadium oxide reduces from the desired oxidation state of 4.01–4.05 to less than 4 in a hydrocarbon rich environment [13,14]. Other authors directly concluded that VPO catalysts as such maybe unsuitable for use in membrane reactor [15], because of poor selectivity in reducing conditions and that a modified formulation, where the phase $(VO)_2P_2O_7$ would be

* Corresponding author. Tel.: +1 514 340 4711x3439; fax: +1 514 340 4159.
E-mail address: gregory-s.patience@polymtl.ca (G. Patience).

0920-5861/$ – see front matter © 2006 Elsevier B.V. All rights reserved.
doi:10.1016/j.cattod.2005.12.013

resistant to reducing conditions, should be developed. Incidentally, the same research group proved that doping VPO with Mo and Co had a promoting effect on the stability of the catalyst [16].

In evaluating a membrane reactor against a traditional fixed bed reactor, another aspect that deserves consideration is the flow distribution. The fixed bed hydrodynamic regime is traditionally characterized as plug flow [17]. Nevertheless, due to non-homogeneities in the packing, radial and angular variations in velocity may be present. These non-homogeneities are difficult to avoid and may give rise to radial velocity variations as a result of higher voidage along the wall: in packed beds the voidage is highest at the wall and then oscillates in a damped fashion until it attains a constant value several particle diameters from the wall.

The voidage profile depends upon the tube diameter (D_t), the particle diameter (d_p) and the particle shape, and models to calculate the voidage in packed beds of spheres are available [18]. The higher voidage at the wall causes the flux, and consequently the velocity, at the wall to increase. Delmas and Froment [19] used the model of Venneth et al. [18] to calculate the velocity distribution in the reaction *o*-xylene to phthalic anhydride by imposing the radial invariance of pressure drop; they predicted that the velocity at the wall may be four to five times higher than in the center of the reactor. Bey and Eigenberger [20] have measured the radial distribution of velocity for a cold flow of air in beds packed with spheres, cylinders and rings, where $3.3 < D_t/d_p < 11$ (aspect ratio) with a superficial velocity of 0.5–1.5 m/s and found that the velocity at the wall may be circa 1.5 times higher than the superficial velocity. Particularly for systems characterized by a low aspect ratio, typical in selective oxidation, the gas flux at the wall may be a significant fraction of the total flux.

Angular variations in the voidage are the result of a non-homogeneous packing and they can also cause significant variation of velocity. These are not well characterized in the open literature and they may depend upon characteristic features of the packing process, for example the type of loading machine [21].

In a recent literature survey, Dixon [6] cited only one study addressing the problem of flow mal-distribution in fixed bed reactor modelling. In this work, Koukou et al. [22] compared the prediction on performance of a H_2-selective membrane reactor for the water gas shift reaction assuming ideal plug-flow and accounting for flow non-idealities. The results clearly pointed out that both CO conversion and H_2 separation are significantly poorer when the flow non-idealities were included. Flow mal-distribution inside the packed bed affects reactor performance by changing the contact time and gas to catalyst volume ratio but it also influences the heat transfer between packed bed and the heat exchange medium.

Using butane partial oxidation as a reaction model, a fluid-bed cooled packed bed membrane reactor with distributed feed of oxygen (air) from the fluid bed to the packed bed was compared to a conventional packed bed. With this membrane configuration we measured a continuously, increasing temperature along the catalytic bed and lower selectivities compared to a fixed bed reactor operating under similar process conditions. Such a temperature profile is characteristic of adiabatic reactors and it indicates that the heat transfer rate between the packed bed in the porous tube and the exterior fluid bed is particularly inefficient. Several potential causes of the increased resistance to heat transfer were identified: (a) low conductivity of the sintered metal constituting the membrane with respect to a compact metal tube; (b) build-up of an insulating solid layer of particles on the fluid-bed side of the membrane wall; (c) enhanced flow mal-distribution in the packed bed side, due to the distributed feed. The scope of this paper is to evaluate each of these resistances and compare the data to that obtained in a fixed bed reactor.

2. Experimental set-up

The experimental system has been described earlier [10]. A schematic diagram of the reactor is shown in Fig. 1. The inlet gas mixture (butane, air and nitrogen) was pre-heated by passing it through a coil in the heated fluid bed. The exit of the coil was connected to the entrance of the membrane at the bottom of the reactor tube. Two configurations were tested: the fixed bed reactor (designated as FR) was made of stainless steel with a 32 mm i.d. and 1 m in length. The membrane reactor (MR) had two sections: the lower section was 500 mm in length and was fabricated from a porous metallic sheet. The upper 500 mm was made of non-porous stainless steel. VPO catalyst was loaded to a height of approximately 500 mm for each configuration. A 17 multipoint thermocouple centered in the catalyst bed monitored the longitudinal temperature profile.

The fluidized bed shell was made of carbon steel with an inner diameter of 127 mm in the lower section that flanged out to 318 mm in the transport disengagement section. Its total length was 1.8 m and a Geldart Group A powder (FCC catalyst)

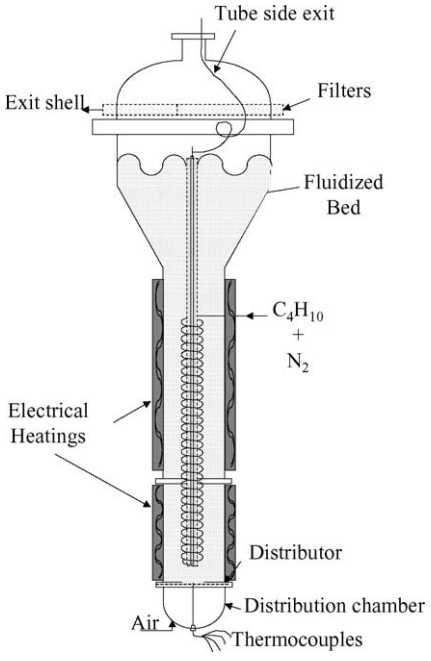

Fig. 1. Membrane reactor diagram.

was used as the fluidizing medium. This fluidized bed was used to control the temperature and, in the case of the membrane reactor, it was a source of oxygen: air from the fluidized bed flows across the porous tube to the VPO catalyst.

The effluent gas stream exited through the top of the reactor and passed through a water quench to condense the product acids. The non-condensable gases were analyzed on-line by a Gas Chromatograph equipped with TCD and FID detectors for O_2, CO, CO_2 and butane. An oxygen paramagnetic analyzer monitored the oxygen concentration in parallel with the GC. The quench was analyzed by HPLC with an ION-300 column. Maleic anhydride (acid) was the main product and other acids included acetic, acrylic, methacrylic, fumaric, and phthalic. Gas exiting was the shell side was monitored with the FID of the GC but no butane was detected indicating that back-permeation was negligible.

3. Results and discussion

Several tests were carried out in both reactors. The entire fixed bed reactor performance data set includes 55 experiments at temperature ranging from 350 to 440 °C, butane concentrations from 0.5 to 1.8%, oxygen concentrations from 5 to 20% and superficial velocities from 0.5 to 0.9 m/s. The membrane reactor performance data set includes 20 experiments where temperature ranged from 350 to 370 °C, overall butane and oxygen concentration from 0.5 to 1.25% and 5 to 20%, respectively, and overall velocities around 0.5 m/s. Permeation flow rate to total flow rate ratios are varied from 0.2 to 0.6.

General observations were described earlier [10]: butane conversion was higher in the membrane reactor compared to the fixed bed but selectivity was lower. In general, the axial temperature profile in the fixed bed reactor was nearly flat. For the membrane reactor, the temperature rose continuously from the entrance to the exit. When both reactors were compared at the same total flow rate, butane and oxygen concentration and fluidized bed temperature—maleic anhydride production was highest in the membrane reactor. However, the average overall temperature was higher in the membrane reactor resulting in higher butane conversion and thus more maleic anhydride even though the overall selectivity was lower. The higher temperature is a result of both the higher conversion but also the lower selectivity. As shown below the heat of reaction of butane to maleic anhydride is less than half that for butane to CO_2.

$$C_4H_{10} + 3.5O_2 \rightarrow C_4H_2O_3 + 4H_2O \quad -\Delta H = 1261\,\text{kJ/mol}$$

$$C_4H_{10} + 6.5O_2 \rightarrow 4CO_2 + 5H_2O \quad -\Delta H = 2659\,\text{kJ/mol}$$

$$C_4H_{10} + 4.5O_2 \rightarrow 4CO + 5H_2O \quad -\Delta H = 1526\,\text{kJ/mol}$$

3.1. Maximum maleic anhydride production

Although butane conversion was lower in the fixed bed reactor compared to the membrane reactor, the temperature profile was flatter. So, it was possible to operate at higher fluidized bed temperatures. The maximum maleic anhydride production rate in the fixed bed (with a 440 °C hot spot temperature constraint), was achieved at a bed temperature of 400 °C with a flow rate of 27 sL/min, and 1.8 and 20 vol.%, butane and oxygen concentration, respectively.

In the membrane reactor, the maximum maleic anhydride production, with the same constraint, was achieved when the operating conditions were: 370 °C fluidized bed temperature, 19 sL/min total flow rate, and butane and oxygen concentrations of 1 and 10 vol.%, respectively.

Fig. 2 shows the temperature profiles along the bed for the fixed bed reactor (FR) and the membrane reactor (MR), and the maleic anhydride production per kilogram of catalyst, at the respective maximum maleic anhydride production rates. The temperature in the fixed bed rose by 30 °C in the first 0.15 m and remained relatively constant thereafter at about 435 °C. The overall average temperature in the fixed bed was at least 25 °C lower than it was in the membrane reactor. The temperature profile in the membrane reactor was very different and increased at a constant rate from the entrance to about 10% from the exit. The maximum temperature recorded was on the same order of magnitude as in the fixed bed reactor at about 440 °C. Due to the higher overall temperature, butane conversion was higher in the fixed bed but the maleic anhydride

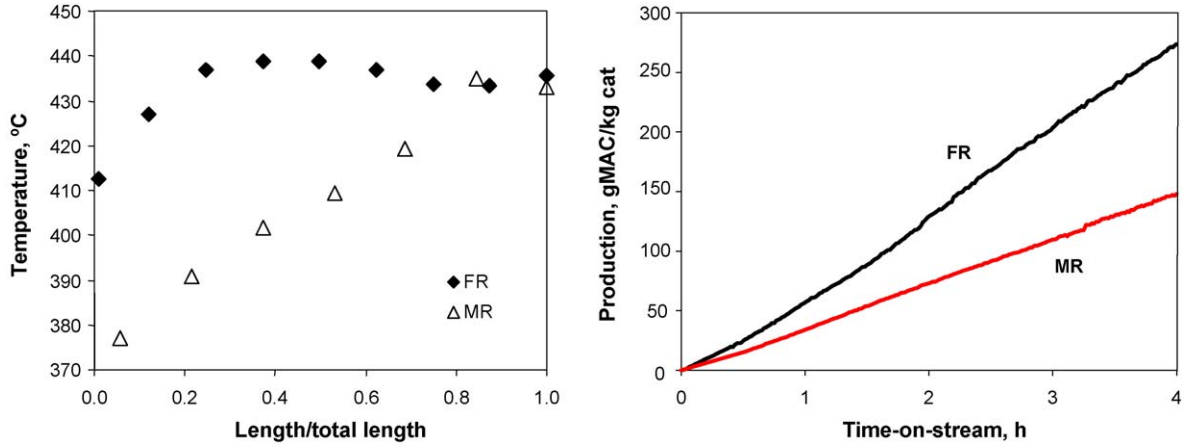

Fig. 2. Temperature profile and maleic anhydride production for the fixed bed (FR) and membrane reactor (MR) at best performance conditions.

selectivity was approximately the same for both reactors. Fig. 2 shows that the higher butane conversion resulted in a higher maleic anhydride production rate by about 50%.

3.2. Constant operating conditions

In the preceding discussion, the reactor performance of the fixed bed and membrane were compared based on the criterion of a 440 °C hot spot temperature. In this section, we compare the reactors based on similar operating conditions: the fluid bed temperature was maintained at 370 °C and the inlet oxygen concentration was 20%. The total flow rate was maintained at 27 sL/min with a permeation flow rate 17 sL/min or a flow ratio of 0.6 (permeate flow to total flow). At this permeation rate, the inlet butane concentration was 1.2% but the mixed cup average concentration would be 0.4%. Comparing fixed bed data with the membrane is complicated due to the change in velocity along the length and the subsequent dilution of the butane. Therefore, to bracket the performance in the "equivalent" fixed bed experiments, we included two conditions: 0.5% butane and 24 sL/min, which corresponded to the mixed cup butane concentration (inlet) and the average flow rate and 1.0% butane and 10 sL/min (overall), which approximated the inlet membrane condition more closely.

The temperature profiles in the fixed bed reactor, shown in Fig. 3, were similar to that shown in Fig. 2: the temperature rose along the first 10% of the bed and then remained constant. The average temperature difference between the two conditions was on the order of 5 °C. The temperature profile along the membrane reactor shown in Fig. 3 was similar to the one in Fig. 2 but with a lower overall temperature rise −30 °C versus 70 °C. The measured maleic production rate in the membrane reactor was slightly higher than in the fixed bed operating at the same inlet conditions and equaled 115 g MAC/kg cat. Butane conversion was almost 50% higher (relative) in the membrane reactor than in the fixed bed, whereas maleic anhydride selectivity was 18% lower (relative).

Fig. 4 shows the evolution of temperature along the bed for the membrane reactor and the fixed bed at the bed entrance and exit. The temperatures overshot the steady state value in both cases by about 5 °C. However, in the case of the exit of the fixed bed, steady state was reached at about 1 h, whereas it takes about 4 h to reach steady state in the membrane reactor. The striking feature of these data, as in the previous section, is that the temperature profile was relatively constant in the fixed bed for both conditions and the temperature increased linearly in the membrane reactor. Since the reaction conditions bracket the conditions of the membrane reactor, the rising temperature is unrelated to the butane concentration or gas velocity. It must therefore be related to heat transfer.

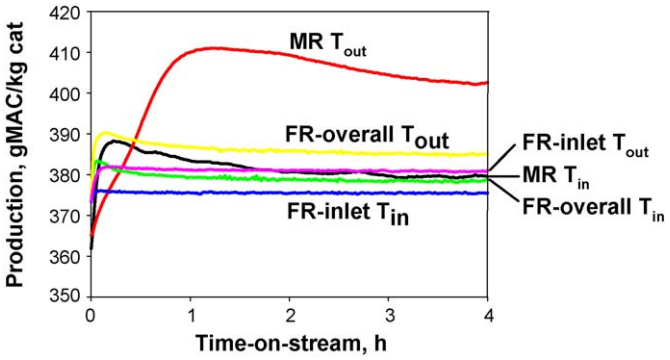

Fig. 4. Temperature evolution with time at the catalyst bed inlet and outlet for membrane reactor (MR) with permeation flow rate to total flow rate ratio of 0.6, and for fixed bed reactor at same overall conditions (FR-overall) and same inlet conditions (FR-inlet).

Generally, the overall heat transfer coefficient in a fixed bed may be approximated by the sum of three resistances: an external resistance between the outer wall and the cooling medium, a conductive resistance across the wall, and an internal resistance between the tube wall and fluid. As mentioned earlier, the void fraction at the wall of fixed beds is higher than the cross-sectional average and therefore, the gas velocity in this region may be significantly greater than the average. This non-uniform velocity profile affects the heat transfer rate. For the membrane reactor configuration, the effect may be more accentuated due to the radial cross-flow.

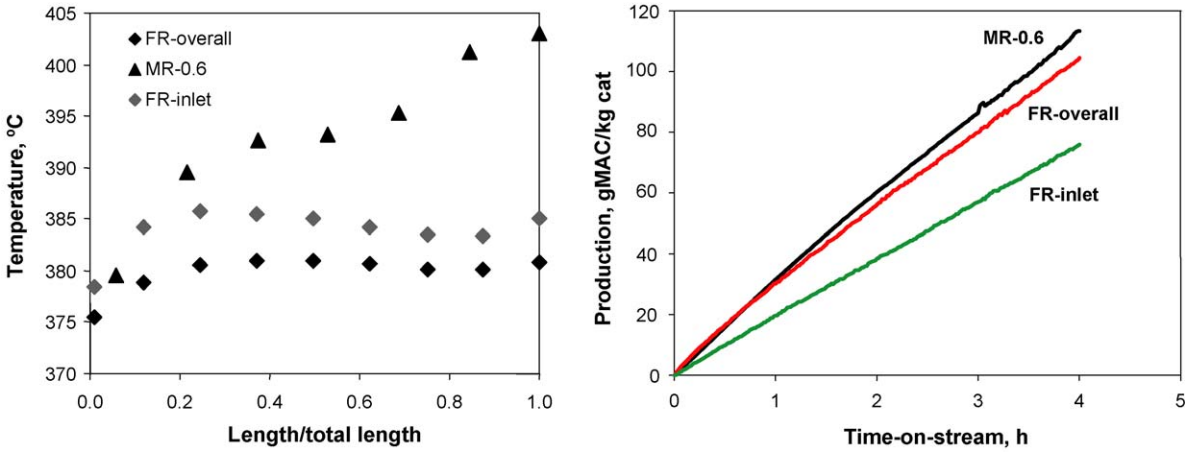

Fig. 3. Temperature profile and maleic anhydride production for the fixed bed reactor at the same overall conditions (FR-overall) and the same inlet conditions (FR-inlet) and the membrane reactor (MR).

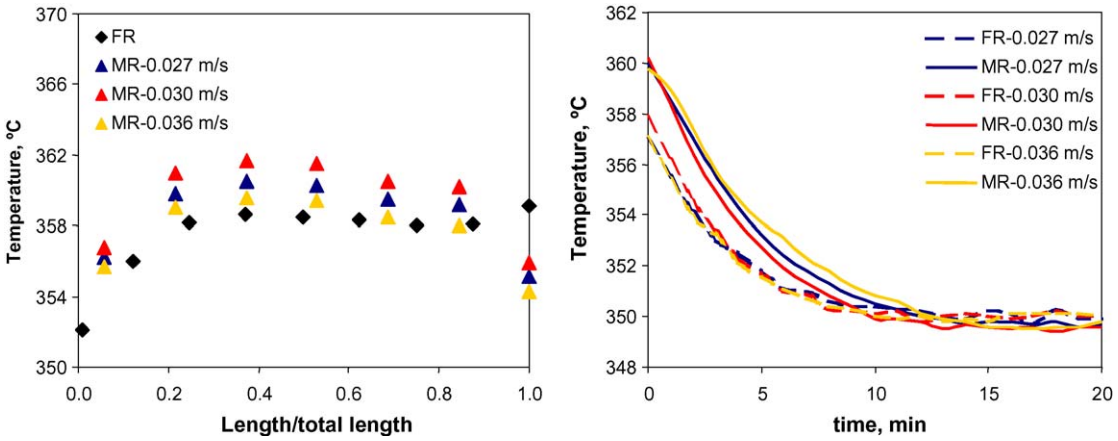

Fig. 5. Temperature profile and temperature decrease with time for the fixed bed reactor (FR) and the membrane reactor (MR) at different fluidization rates.

3.3. Tube thermal conductivity

Besides hydrodynamics, the thermal resistance of the reactor tubes is an obvious difference between the two configurations. In order to gauge the membrane thermal resistance versus the fixed bed reactor tube, we operated the membrane reactor in the fixed bed regime: The pressure differential between the membrane and fluid bed was set to zero resulting in zero cross flow. All flow was introduced at the entrance of the membrane. Under these conditions the temperature profile with the porous tube was equal to that observed with the standard tube. As shown in Fig. 5, the steady state axial velocity profile is essentially flat across most of the bed (except at the entrance and the exit where the porous membrane is welded to a stainless steal pipe). The time it takes the temperature to achieve steady state after the butane feed is interrupted is also the same. Clearly, the thermal conductivity of the porous tube is sufficiently high and, therefore, the poorer heat transfer rate must be due to hydrodynamic phenomena.

3.4. Solids build-up on the outer wall, h_{fb}

Porous metallic tubes are commonly used for separating particulates from gas streams that pass through cyclones. With time, the filters become blocked with fine powder ($d_p < 15$ μm) and they are cleared by applying a high gas flow in the reverse direction: blow-back. Eventually, the blow-back cycle becomes less efficient and the filters block and require a chemical cleaning. In the present configuration, the face velocity across the outer surface of the membrane is significantly less than velocities typical of filter operations and the average particle size is also much larger (70 μm). After several months of operation, the pressure differential across the membrane has remained constant indicating that pores remain clear of ultra fine particles.

Besides pore blockage, another phenomenon that may limit heat transfer is that due to the build up of a layer of solids along the membrane wall. Heat transfer rates in fluidized beds are very high because of frequent collisions between the solids and the solids surface—solids residence times are short and as a result the heat transfer coefficient is on the order of 600 W/m^{2}K [25]. However, in the membrane reactor, the radial gas velocity at the wall equals 0.004 m/s, which is greater than minimum fluidization velocity and may cause particles to adhere to the wall for a longer period of time and thus reduce the contact frequency. This tendency to adhere is counteracted by the shear caused by the motion of solids and gas in the fluid bed.

The overall heat transfer coefficient (U) is composed of the individual resistances of the fluid bed to outer wall (h_{fb}), thermal conductivity of the tube ($d_i \ln(d_o/d_i)/2\lambda$), inner wall to fluid ($h_w$) and finally fluid to particle (h_p) (see Fig. 6):

$$\frac{1}{U} = \frac{1}{h_{fb}} + \frac{d_i \ln(d_o/d_i)}{2\lambda} + \frac{1}{h_w} + \frac{1}{h_p} \quad (1)$$

where d_i = 34 mm, wall thickness = 0.154 mm, and λ = 21 W/m K for stainless steel.

Based on the transient response data in the fixed bed, the overall heat transfer co-efficient was on the order of 100 W/m^2 K, which it is nearly equal to the one calculated by other researches in fixed bed reactors similar to this one [26]. The resistance due to thermal conductivity represents approxi-

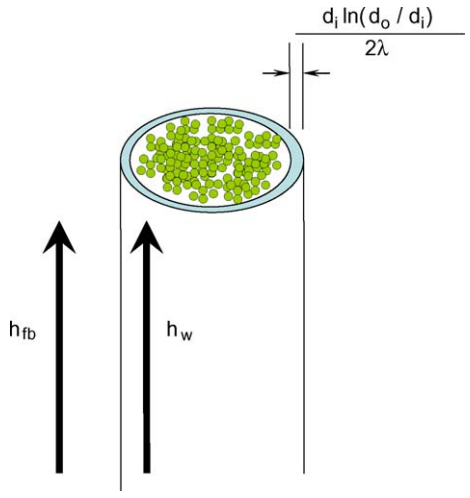

Fig. 6. Schematic of the major heat transfer resistances.

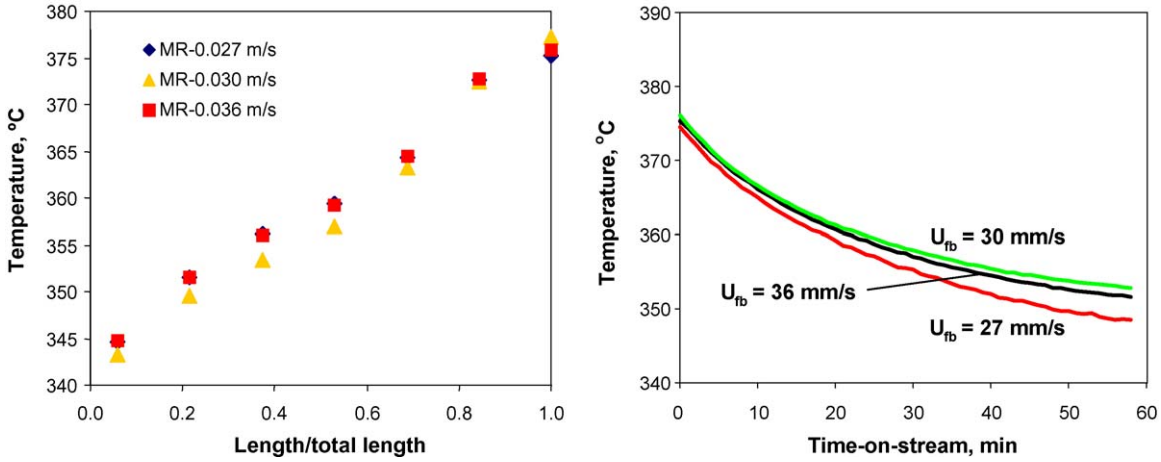

Fig. 7. Steady and transient temperature profiles in the membrane reactor (MR) at different fluidization flow rate. Fluid bed temperature 350 °C, 19 sL/min total flow rate, 19 sL/min permeation rate, butane and oxygen concentrations of 1 and 20%, respectively.

mately less than 1% of the total resistance, 16% is attributable to the fluid bed-wall resistance, therefore, the other 83% is due to the resistance between the inside wall and the fluid (we have also neglected the particle-fluid resistance). The overall resistance in the membrane reactor is approximately ten times lower than that of the fixed bed. This drop may be due to a combination of h_{fb} and h_w since we have already demonstrated that it is unlikely that it is due to the difference in thermal resistance of the tube.

Several experiments were conducted in which the gas flow rate to the fluid bed was varied while maintaining the operating parameters of the membrane reactor unchanged. These tests were designed to assess the relationship between the fluidized bed gas velocity and the heat transfer rate. The superficial gas velocity was varied from 27 to 36 mm/s, which represents from 13 to 18 times the minimum fluidization velocity ($13 < U/U_{mf} < 18$). The membrane reactor operated with 1% butane, 10% oxygen and 350 °C and a flow ratio of 0.5.

Fig. 7 illustrates both the steady state temperature profile and the transient. Differences in the temperature profile for each of the three different gas rates in the fluid bed are within the experimental error. This suggests that the gas rate in the fluidized bed had no effect on the heat transfer rate in the range tested. However, only a narrow range of gas velocities were tested and further experiments are required with higher gas velocities. The fluid bed was operating in the bubbling fluidization regime and we may expect a different result in the turbulent fluidization regime where the gas flow rates would be as much as twenty times higher. Future studies should also be conducted with higher density powders or particles with a larger diameter to evaluate their effect.

3.5. Internal resistance—h_f

The last set of experiments examines the effect of tube side Reynolds number on heat transfer. As mentioned previously, several studies have shown that the void fraction at the wall is higher than the cross-sectional average. Recently, Nguyen et al. [27] measured the radial oscillations in porosity using magnetic resonance imaging. For cylinders with similar dimensions used in this study, they reported a wall voidage of 70%. The oscillation damped to within 10% of the mean porosity (0.035) after 3 particle diameters. Assuming that the radial pressure gradient is close to zero, the gas velocity at the wall is necessarily higher than in the average to maintain a similar axial pressure drop profile. This high porosity region may allow gas permeating across the membrane to short circuit the bed of solids and preferentially flow up the wall, which may impact the heat transfer rate considerably.

An extensive body of literature covers the topic of heat transfer in conventional packed beds including systems with low aspect ratio. Particularly for these systems, Dixon and co-workers [28–30] have compared several correlations and experimental data and proposed new correlations for some of the key parameters of the heat transfer models. Dixon and co-workers [28,29] discuss the effect of D_t/d_p and Re on the various components of Pe_r. The wall to fluid Nusselt number and the wall to solid heat transfer coefficient (Bi_s) are affected by D_t/d_p. Later, Derckx and Dixon [31] compared various choice of the wall Nusselt number and concluded that correlations including the effect of D_t/d_p are definitely to be preferred at low Re (demonstrated in the paper for $Re < 60$), and the influence of D_t/d_p on Nu_w becomes less and less significant when Re increases. In general, most correlations show that the heat transfer rate increases at most proportionately with Reynolds number. Based on the correlations presented by Wellauer et al. [26], the heat transfer coefficient rises only 25% when doubling Re from 40 to 80. Nevertheless, we tested the effect of increasing the Reynolds number on heat transfer hoping that the higher gas velocity might improve the radial mixing.

The experimental procedure consisted of generating a temperature differential across the bed and then interrupting the butane feed rate and simultaneously doubling the tube flow rate. Flow ratios between 0.15 and 0.6 were tested and the data for the last thermocouple in the bed are shown in Fig. 8. The dashed lines represent the change in temperature with a flow rate of 20 N L/min and the solid lines represent 40 N L/min (exit Re equals 86 and 127, respectively). The time it takes the

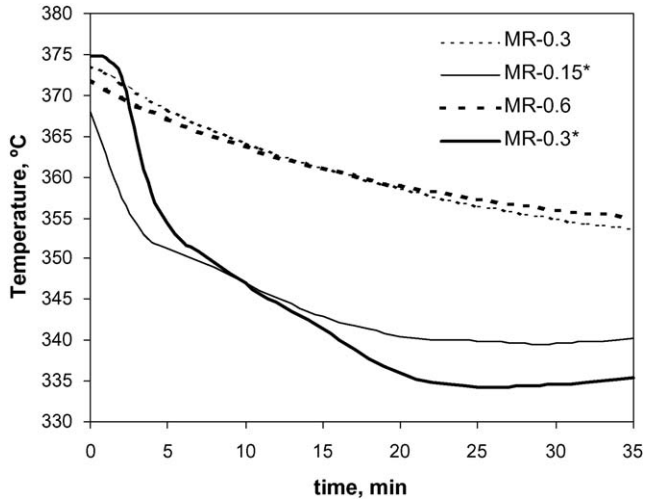

Fig. 8. Temperature decrease with time in the membrane reactor at total flow rates of 20 N L/min (dash line) and 40 N L/min (solid line) and at different permeation flow rate to total flow rate ratios.

thermocouple to reach the steady state value is considerably shorter at a flow rate of 40 N L/min compared to 20 N L/min, which confirms the importance of radial mixing. It took approximately 1 h to reach the fluid bed temperature at a flow of 20 N L/min, compared to about 20 min with a flow rate of 40 N L/min. Further investigation is required to assess the effect of flow ratio on heat transfer. As the flow ratio approaches zero (fixed bed conditions) the heat transfer rate should approach that of a fixed bed.

4. Conclusions

Membrane reactor technology has several advantages versus conventional fixed bed technology. By separating the oxidant from the hydrocarbon the process is inherently safer. Furthermore, oxygen (or hydrocarbon) may be fed in an optimal way to maintain catalyst activity but reduce parasitic parallel and series reactions. However, data presented in this work show that, on average, the overall performance in the conventional fixed bed is superior to the membrane configuration because selectivity is higher and the reactor may be operated at higher temperatures resulting in superior MA yields. The reason for the large difference in performance was partially attributable to the poorer heat transfer rate in the membrane reactor. The internal resistance from the wall to fluid in the membrane appeared to be significantly higher than the fixed bed. A likely mechanism to account for the poorer heat transfer is that gas permeating across the membrane flows preferentially up the inner wall. Increasing the Reynolds number by doubling the tube side flow rate increased the heat transfer rate to values approaching the fixed bed.

Acknowledgment

The authors gratefully acknowledge the financial and technical support from Haldor Topsøe A/S.

References

[1] J.G.S. Macano, T.T. Tsotsis, Catalytic Membranes and Membrane Reactors, Wiley/VCH, Weinheim, 2002.
[2] G. Saracco, H.W.J.P. Neomagus, G.F. Veersteeg, W.P.M. van Swaaij, Chem. Eng. Sci. 54 (1999) 1997.
[3] K.K. Sirkar, P.V. Shanbhag, A.S. Kovvali, Ind. Eng. Chem. Res. 38 (1999) 3715.
[4] A. Julbe, D. Farrusseng, C. Guizard, J. Mem. Sci. 181 (2001) 3.
[5] J. Coronas, J. Santamaría, Catal. Today 51 (1999) 377.
[6] A.G. Dixon, Int. J. Chem. Reac. Eng. 1 (2003), Review R6.
[7] M. Alonso, M.J. Lorences, M.P. Pina, G.S. Patience, Catal. Today 67 (2001) 151.
[8] F. Klose, T. Wolff, S. Thomas, A. Seidel-Morgenstern, Catal. Today 82 (2003) 25.
[9] A.L.Y. Tonkovich, J.L. Zilka, D.M. Jimenez, G.L. Roberts, J.L. Cox, Chem. Eng. Sci. 51 (1996) 789.
[10] M. Alonso, M.J. Lorences, G.S. Patience, A.B. Vega, F.V. Díez, S. Dahl, Catal. Today 104 (2005) 177.
[11] R. Mallada, M. Pedernera, M. Menéndez, J. Santamaría, Ind. Eng. Chem. Res. 39 (2000) 620.
[12] M. Pedernera, R. Mallada, M. Menéndez, J. Santamaría, AIChE J. 46 (2000) 2489.
[13] G. Centi, G. Fornasari, F. Trifirò, J. Catal. 189 (1984) 44.
[14] R. Mallada, S. Sajip, C.J. Kiely, M. Menéndez, J. Santamaría, J. Catal. 196 (2000) 1.
[15] S. Mota, M. Abon, J.C. Volta, J.A. Dalmon, J. Catal. 193 (2000) 308.
[16] S. Mota, J.C. Volta, G. Vorbeck, J.A. Dalmon, J. Catal. 193 (2000) 319.
[17] O. Levenspiel. Chemical Reaction Engineering, John Wiley and Sons, ISBN 0-471-25424-X.
[18] M.H. Venneth, V.M.H. Govindarao, G.F. Froment, Chem. Eng. Sci. 41 (1986) 533.
[19] H. Delmas, G.F. Froment, Chem. Eng. Sci. 43 (1988) 2281.
[20] O. Bey, G. Eigenberger, Chem. Eng. Sci. 52 (1997) 1365.
[21] M.F. Mathias, G.P. Muldowney, Chem. Eng. Sci. 55 (2000) 4981.
[22] M.K. Koukou, M. Papayannakos, N.C. Markatos, Chem. Eng. J. 83 (2001) 95.
[25] S.A.R.K. Deshmukh, M.v.S. Annaland, S. Volkers, H. Kuipers, Int. J. Chem. Reac. Eng. 3 (2005) A1.
[26] T. Wellauer, D.L. Cresswell, E.J. Newson, ACS Symp. Ser. No 196 (1982) 527.
[27] N.G. Nguyen, V. van Buren, R. Reimert, A. von Garnier, Magn. Res. Imag. 23 (2005) 395.
[28] A.G. Dixon, M.A. DiCostanzo, B.A. Soucy, Int. J. Heat Mass Transf. 27 (1984) 1701.
[29] M.M. Melanson, A.G. Dixon, Int. J. Heat Mass Transf. 28 (1985) 383.
[30] A.G. Dixon, J.H. Van Dongeren, Chem. Eng. Process. 37 (1998) 23.
[31] O.R. Derckx, A.G. Dixon, Catal. Today 35 (1997) 435.